SANDIA REPORT

RECEIVED
DEC 15 1997
OSTI

Synthetic Molecular Receptors for Phosphates and Phosphonates in Sol-Gel Materials

DISTRIBUTION OF THIS DOCUMENT IS UNLIMITED

Darryl Y. Sasaki, Todd M. Alam, Roger A. Assink, Charles E. Daitch, Carol S. Ashley, C. Jeffrey Brinker, Joseph S. Schoeniger, Diana C. Roe, Phillip I. Pohl, Daniel J. Rush, Kenneth J. Shea

MASTER

Sandia National Laboratories

DISCLAIMER

Portions of this document may be illegible
in electronic image products. Images are
produced from the best available original
document.

Synthetic Molecular Receptors for Phosphates and Phosphonates in Sol-Gel Materials

Darryl Y. Sasaki, Todd M. Alam, Roger A. Assink, and Charles E. Daitch
Materials Aging & Reliability Bulk Properties Department

Carol S. Ashley and C. Jeffrey Brinker
Direct Fabrication Technologies Department

Joseph S. Schoeniger and Diana C. Roe
Exploratory Systems Technologies

Phillip I. Pohl
Environmental Risk & Regulatory Analysis

Sandia National Laboratories
P.O. Box 5800
Albuquerque, New Mexico, 87185-1407

Daniel J. Rush and Kenneth J. Shea
University of California, Irvine
Department of Chemistry
Irvine, California 92717

Abstract

Synthetic receptors for phosphates and phosphonates have been generated in SiO_2 xerogels via a surface molecular imprinting method. The monomer 3-trimethoxy silylpropyl-1-guanidinium chloride (1) was developed to prepare receptor sites capable of binding with substrates through a combination of ionic and hydrogen bond interactions. HPLC studies and adsorption isotherms performed in water have found that molecular imprinting affords a significant improvement in K_a for phosphate and phosphonate affinity over a randomly functionalized xerogel. Affinities for these materials offer about an order of magnitude improvement in affinity compared to analogous small molecule receptors reported in the literature. The xerogel matrix appears to participate in host-guest interactions through anionic charge buildup with increasing pH.

Acknowledgment

Contents

Figures

Tables

Synthetic Molecular Receptors for Phosphates and Phosphonates in Sol-Gel Materials

Introduction

The selective and rapid detection of phosphate and phosphonate compounds, which include numerous biologically important signaling molecules (1-3) as well as pesticides and chemical warfare agents (4), is dependent upon the development of efficient host-guest systems. Various solution phase synthetic molecular host-guest systems have been developed to selectively bind phosphate esters using hydrogen bonding and electrostatics to achieve high affinity (5-9). A major drawback is the inability of these systems to achieve high complexation in the presence of water, a situation in which the detection of these compounds is desired. In contrast to these small molecule hosts, self-assembled Langmuir monolayers with guanidine functionality have produced some high binding constants for nucleotides in water through guanidine-phosphate pairing (10). It is believed that the monolayer host systems have some uniquely structured water near the interface that enhances host-guest binding, a feature non-existent for small molecule systems which operate in bulk water. Molecular receptors embedded in polymer scaffolds, like proteins, may offer interfacial reordering of water near the receptor that could enhance substrate binding (11,12). Although it is unclear how to mimic proteins in this regard, efforts into the design and preparation of molecular receptors on polymer matrices may lead to the development of molecular recognition materials with enhanced selectivity and sensitivity under aqueous conditions.

Successful preparation of synthetic receptors in crosslinked polymers via the molecular imprinting methodology has generated a broad range of materials with molecular recognition properties (13). This method has already demonstrated that some highly selective receptor sites can be built for complex molecules, such as sugars (14), amino acids (15), peptides (16), nucleosides (17), and others, in polar organic solvents. Some strides in binding affinity for host-guest interactions in aqueous solution have been made in recent years (18, 19). However, selectivity and affinity in the presence of water remains a problem in these organic based materials.

We describe herein a new silica sol-gel molecular imprinted material for aqueous phase recognition of phosphate and phosphonate substrates. The receptors are functionalized with the guanidine moiety which provides specific points of interaction in the aqueous environment. The guanidine residue was chosen for its ubiquitous presence in protein receptors sites often acting as the main interaction point for phosphate compounds (20). The guanidinium-phosphate interaction employs a combination of electrostatic as well as bidentate hydrogen bonds to achieve high recognition properties (21). Guanidine alkyl silanes were used to functionalize the silica matrix formed by a sol-gel process. Previous studies of imprinting in silica gels have demonstrated that metal oxides can provide for good affinity and selectivity of guest substrates in organic and aqueous solutions (22-26). The sol-gel process for molecular imprinting introduced here offers the

ability of designing and building the material's matrix starting at the molecular level allowing facile tailoring of the material's polarity, pore dimension, and surface functionalization. Additionally, silica sol-gels offer many desirable features as the scaffold for molecular receptor sites which include a hydrophilic surface, optical transparency (for applications as sensor materials), and a highly crosslinked, robust structure with high surface area.

Experimental

General. Silane reagents were obtained from Gelest, Inc. Reagent 3-Amino-1-trimethoxypropylsilane was distilled prior to use. Water was purified through a Barnstead Type D4700 NANOpure Analytical Deionization System. 1-H-pyrazole-1-carboxamidine hydrochloride reagent was prepared by the reported procedure (*27*). Solution phase ^{1}H, ^{13}C, and ^{31}P NMR experiments were performed on a Bruker AM300 NMR spectrometer, and infrared spectra were obtained on a Perkin-Elmer 1750 FTIR spectrophotometer. Mass spectroscopy was performed by Mass Consortium, Corp.

1-Trimethoxysilylpropyl-3-guanidinium chloride (1). A solution of 3-amino-1-trimethoxypropylsilane (10.0 g, 55.8 mmole) and 1-H-pyrazole-1-carboxamidine hydrochloride (8.20 g, 55.9 mmole) in dry methanol (30 mL) was stirred for 15 hours at room temperature. The solvent was removed in *vacuo* leaving a viscous, colorless oil which was purified by Kugelrohr distillation (150 °C, 100 μmHg) to remove the pyrazole byproduct. A clear, colorless, viscous oil of the product **1** remained (12.7 g, 88%). ^{1}H NMR (CDCl$_3$) δ 7.83 (t, J = 6.5 Hz, 1H, CH$_2$N*H*), 7.07 (br s, 4H, N*H*$_2$), 3.58 (s, 9H, OC*H*$_3$), 3.20 (dt, J = 6.5, 6.5 Hz, 2H, NHC*H*$_2$), 1.72 (m, 2H, C*H*$_2$), 0.72 (t, J = 7.8 Hz, 2H, Si-C*H*$_2$). ^{13}C NMR (CDCl$_3$) δ 157.75, 50.59, 43.31, 22.42, 5.83. IR (NaCl) 3330, 3166, 2946, 2850, 1652, 1469, 1192, 1083, 819 cm^{-1}. High resolution MS calcd for C$_7$H$_{20}$N$_3$O$_3$Si: 222.1274. Found: 222.1281.

Xerogel Preparation. Ethanol (305 mL) and tetraethoxysilane (305 mL) were stirred in a 1 L vessel followed by the addition of water (24.5 mL) and 1N aqueous HCl (1 mL). The mixture was warmed to 60 °C with stirring for 1.5 hours, then cooled to room temperature to afford the homogeneous sol solution. To the sol (91 mL) was added 0.1 M aqueous NH$_4$OH (9.1 mL). The solution gelled overnight and was aged in a closed container at 50 °C for one day. The gel was then crushed, washed with ethanol twice, collected, placed in fresh ethanol (200 mL), and kept at 50 °C overnight. For molecular imprinting the gel was collected and placed in a 100 mL solution of ethanol containing **1** (8.0 mmole) and phenylphosphonic acid (4.0 mmole) template and the mixture incubated for another day at 50 °C. The solvent was subsequently evaporated at 50 °C over a period of 12 hours. Blank and randomly functionalized xerogels were prepared identically with the exclusion of **1** and phenylphosphonic acid (PPA) for the blank gel and of PPA for the randomly functionalized gel. The xerogel was then crushed to a 75-250 micron particle size,

washed with ethanol, and dried under vacuum at 60 °C for a day. Prior to rebinding or HPLC studies, all materials were washed three times with 1 N aqueous HCl solution (100 mL/g xerogel) by swirling one hour for each wash at room temperature. The gels were then washed liberally with pure water followed by drying under vacuum at 60 °C overnight. Quantitative removal of the PPA template was determined by UV analysis (PPA in 50% methanol/1 N aqueous HCl, $\varepsilon = 8332$ at 210 nm).

HPLC Analysis. Xerogels processed to a particle size of 25-38 μm were slurry packed into a 4.6 mm i.d. x 100 mm HPLC column which was connected to a Waters 600-MS HPLC fitted with a Waters 484 tunable wavelength UV detector set at 260 nm. All studies used a mobile phase consisting of 95% aqueous buffer solution/5% acetonitrile. The ionic strength dependence study used an aqueous buffer composed of 0.01 M potassium phosphate adjusted to pH 6.0 with either HCl or KOH, and the ionic strength was adjusted to the appropriate value by the addition of KCl. The pH dependence study used an aqueous buffer composed of 0.01 M potassium phosphate adjusted to the appropriate pH with either HCl or KOH, where the ionic strength was maintained at 0.05 M with the addition of KCl. Capacity factors for Figure 5 were determined using acetone as the void volume marker, an aqueous phase of 0.01 M potassium phosphate buffer adjusted to pH 6.0 or 8.0, and ionic strength of 0.05 M.

Rebinding Studies. Xerogel (50 mg) at 75-150 μm particle size was placed in a solution containing a phosphate or phosphonate substrate at various concentrations in a volume such that the total bound substrate in the xerogel amounted to less than 10 mole % of the total substrate in solution. The pH of the solution was adjusted to ~5 using the substrates as the buffering medium. Although the solution equilibrates with the xerogel in minutes the solution was swirled overnight prior to analysis. An aliquot was taken from the solution and analyzed for depletion by an acid molybdate/Fiske & SubbaRow reducer assay (Sigma Chemicals) for PO_4 or by ^{31}P NMR for PPA. The binding data were evaluated by Scatchard analysis giving linear plots over the concentration range of 1 - 10 mM. Binding constants (K_a) and binding capacities (guanidine:substrate) are reported in Table II.

Solid State NMR. Direct polarization ^{29}Si solid state MAS NMR spectra were recorded on a Bruker AMX 400 spectrometer at a resonant frequency of 79.500 MHz using a 7 mm bb MAS probe and a 4 kHz spinning speed. The reference was external Q_8M_8 ($\delta = 11.5$ ppm). These spectra were recorded with a delay time of 300 seconds which is several times longer than the relaxation times of the sample to ensure quantitative spectra of the Q silicon species, where $Q^n = Si(OSi)_n(OR)_{4-n}$. Cross-polarization [29]Si spectra of the 4% xerogel were recorded at 39.7 MHz on a Tecmag console interfaced to a Chemagnetics spectrometer. A 7 mm MAS probe, a 3.5 kHz spinning speed, a contact time of 6 ms and a delay time of 4 seconds were used. The cross-polarization time was chosen so that the T resonances and the Q^2 and Q^3 resonances were expected to be quantitative. The resonances of the Q and T silicon species were deconvoluted using

Gaussian components to calculate the extents of reaction and the relative amounts of Q and T silicons.

Results and Discussion

The molecular imprinting technique employed for the sol-gel materials allowed surface functionalization of the matrix to maximize accessibility of receptor sites while minimizing structure modification of the gel matrix. A SiO_2 xerogel was first prepared from tetraethoxysilane using a standard literature procedure for sol-gel processing (28). The xerogel was functionalized with the guanidine siloxane monomer, 3-trimethoxysilyl propyl-1-guanidinium chloride (1), prepared by reaction of 1-trimethoxysilylpropyl-3-amine with 1-H-pyrazole-1-carboxamidine hydrochloride. The siloxane monomer 1 was condensed onto the silica surface in ethanol solution in the presence of the template molecule, phenylphosphonic acid (PPA), in a 2:1 ratio to generate a receptor site as ideally illustrated in Figure 1. The finished material was dried, gently ground, and sieved to appropriate size.
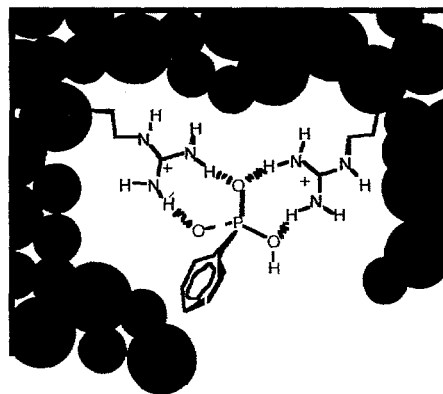

Figure 1. Idealized Bis-guanidine Receptor Site for Phosphonate.

Materials Characterization

Structural information for the xerogels was obtained through ^{29}Si solid state MAS NMR providing quantitative determination of the extent of condensation of the matrix and functionalization with 1. Direct polarization ^{29}Si NMR was used to quantify the Q, or $Si(OR)_4$, species in the silica gel, where R = Si, H, or ethyl (29). From the abundance of various Q species the extent of condensation of matrix silica could be determined. The blank xerogel was found to have $90 \pm 1\%$ condensation indicating high crosslinking. A comparison of blank xerogel and xerogel functionalized with 1 showed that 1 to 4 mole % functionalization does not affect condensation of the gel matrix. Cross-polarization experiments measuring the T silicon $(SiR'(OR)_3$, where R = Si, H, or ethyl and R' = propyl-3-guanidinium) of covalently bound 1 determined an incorporation of 1 into the gel at $93 \pm 10\%$ with an extent of condensation of $91 \pm 2\%$. Thus, the procedure used for surface functionalization was successful with near quantitative coupling of siloxane monomer to the matrix and an approximate three point covalent attachment.

Surface area analyses were performed to determine any gross structural changes that might occur upon guanidine functionalization of the xerogel surface. Table I shows nitrogen BET analyses of blank xerogel and gels randomly functionalized with 1 at 2% and 4%, and an imprinted gel with 4% of 1 and PPA imprinting at a 2:1 ratio of guanidine to PPA. The percentages of 1 are

9

indicated as a mole percent relative to total silicon in the gel. With 2% functionalization the xerogel shows only a slight increase in surface area to 915 m²/g over the non-functionalized material (876 m²/g) but a 65% increase in pore volume. Upon further functionalization to 4%, the surface area drops appreciably (836 m²/g) along with pore volume. Addition of the PPA template brings about a further decrease in surface area while pore volume remains constant. Overall the functionalization process does not significantly alter the xerogel structure, however, some trends were observed. Most noticeable is that surface functionalization with **1** leads to an increase in pore volume of 35-65%. Since **1** can act as a capping agent for surface silanols, surface functionalization could minimize condensation across walls of collapsing pores leading to higher pore volumes for functionalized xerogels (*30*). We can offer no good explanation as to why the surface area decreases as functionalization increases from 2 to 4% and further with PPA imprinting. With an average calculated area per bound guanidine of 225 Å², site isolation is highly probable assuming random distribution.

Table I. BET Surface Area Analysis

% 1/SiO$_2$	Template molecule	Surface area (m²/g)	Pore volume (cm³/g)
0	none	876	0.63
2	none	915	1.01
4	none	836	0.86
4	PPA	771	0.85

Host-guest Interactions

   Ionic Strength. In an effort to understand host-guest interactions of phosphate and phosphonate substrates to these sol-gel materials, several HPLC studies were performed. Relative affinities of a phosphonate diester and a phosphonic acid to blank and randomly functionalized 4% guanidine xerogels were measured in an ionic strength study to qualitatively determine the contribution of ionic interaction between the host and guest. The eluent used was a solvent mixture of 95% 0.01 M potassium phosphate buffered water at pH 6.0 and 5% acetonitrile. The ionic strength was adjusted with KCl. Specific interaction of the guanidines with the phosphonic acid substrate should involve a combination of electrostatics and hydrogen bonding. On the other hand, binding of phosphonate diester would occur solely through hydrogen bonds. Figure 2 shows the effect of ionic strength on retention time to blank and functionalized gels with acetone, diisopropylphenylphosphonate (DIPP), and phenylphosphonic acid (PPA) substrates. Increasing ionic strength is indicated with increasing darkness of the bar. Acetone, which has no specific

10

interaction to the materials, shows essentially no difference in affinity to both gels and no effect due to changes in ionic strength. DIPP exhibits a high non-specific affinity to the blank xerogel, but this affinity diminishes upon functionalization of the gel. Conversely, PPA shows no affinity for the blank gel, but high affinity for the 4% guanidine gel. Functionalization of the gel with **1**
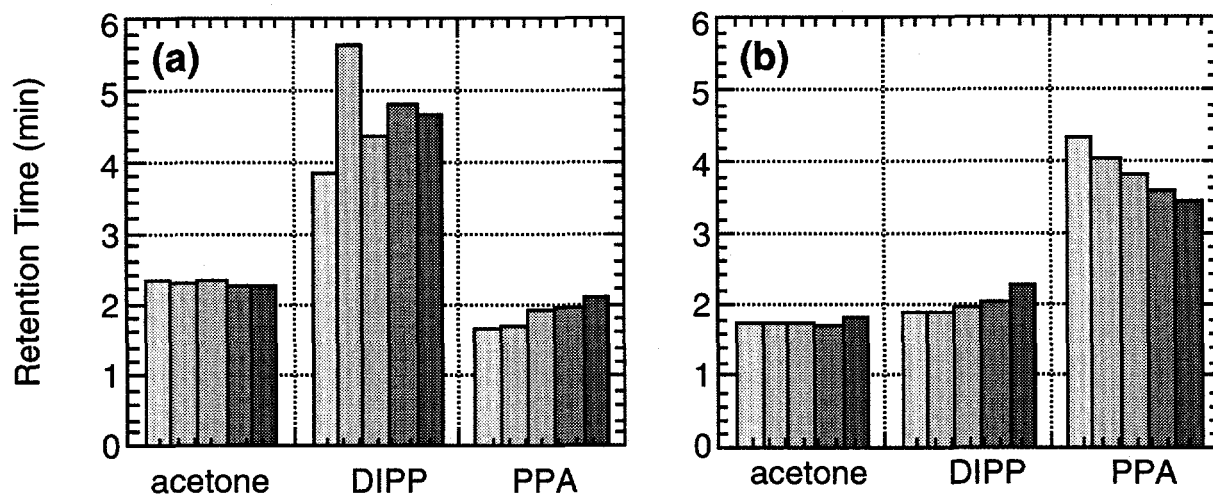

Figure 2. HPLC Study of the Effect of Ionic Strength on Substrate Affinity to Blank and Functionalized Xerogel. Graphs are of data from blank (a) and 4% guanidine (b) xerogels. The ionic strength increases from left to right above each substrate from 0.02, 0.05, 0.10, 0.20, to 0.50 M.

effectively minimizes non-specific interaction of phosphonate esters while adding specificity for phosphonic acids. The effect of ionic strength on the affinity of PPA to 4% guanidine gel shows a trend of reduced affinity with increasing ionic strength. This is an expected observation for phosphonate-guanidine complexation where ionic pairing contributes to the binding interaction. Guanidine-phosphonate pairing has an additional hydrogen bond component which is believed to provide coordination of substrates in protein receptor sites (*11*). It is possible that hydrogen bonding also actively participates in these synthetic receptors and is responsible for the affinity observed at higher ionic strengths. From the data, however, it is evident that hydrogen bonding between DIPP and guanidine is negligible under the aqueous conditions.

Effect of Solution pH. HPLC studies on the effect of pH on substrate retention time shows a trend of diminishing affinity with increasing pH. The mobile phase in these studies was a 5% acetonitrile/95% aqueous phosphate buffer solution adjusted to the desired pH, and ionic strength held at 0.05 with added KCl. Figure 3 shows a comparison of blank and guanidine functionalized xerogel run with acetone, DIPP, and PPA at several pH values from 2 to 10. The retention time of acetone is unaffected by changes in pH or gel type. For the phosphonate substrates, however, DIPP on the blank gel and PPA on functionalized gel show an inverse relationship between retention time (affinity) and pH. Moreover, a complete loss of affinity is
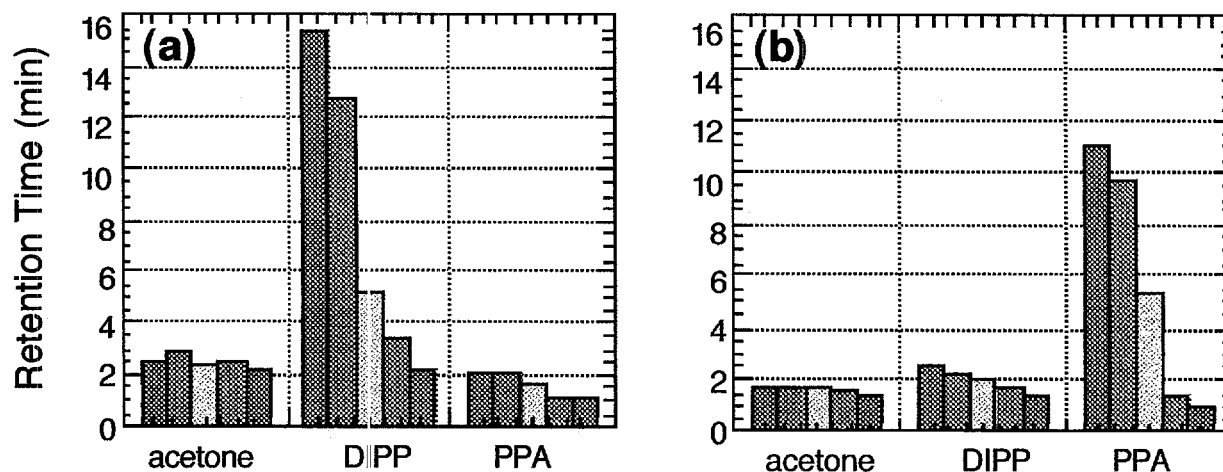
Figure 3. HPLC Study of the Effect of pH on Substrate Affinity on Blank and Functionalized Xerogels. Graphs are of data from blank (a) and 4% guanidine (b) xerogels. The pH increases from left to right in the order of 2.0, 4.0, 6.0, 8.0, and 10.0.

found at pH 8 and above. In considering the specific interaction of the guanidine functionalized gel with PPA, strongest host-guest interactions should be found near neutral pH. However, the data show that highest affinity is found at the lower pH values. The PPA affinity appears to be influenced by the extent of deprotonation of the acidic silanol groups on the silica matrix producing an increasingly anionic surface above pH 2. Although the guanidine group can specifically bind with PPA the silica matrix dominates substrate interaction with changing solution pH. Figure 4 illustrates the possible host-guest-matrix interaction at low and high pH. At low pH the silica surface will be close to neutral charge allowing the guanidinium group to bind freely with PPA. At higher pH a negatively charged surface could force the cationic guanidinium to interact with the surface and restrict binding with the PPA guest (Figure 4). Other contributions for poor affinity at high pH could arise from ionic repulsion between the matrix and substrate or surface effects which may lower the pK_a of guanidinium (13.6 in water) thereby minimizing electrostatic interactions with PPA at pH's lower than predicted. For the phosphonate diester DIPP it is unclear why there is a pH dependent non-specific interaction to the blank gel although reasonable explanations, which are out of the scope of this text, involving polar interactions with the surface could be made. Functionalization of the gel with 1, however, appears to remove the non-specific affinity at all pH levels.

An HPLC study comparing imprinted vs randomly functionalized 4% guanidine xerogels is shown in Figure 5. The two graphs present a comparison of capacity factors for DIPP and PPA to the xerogels at two different pH values of 6 and 8. At pH 6, PPA shows a modest, yet

12

significantly higher, affinity for the imprinted material with a 25% increase in the capacity factor over the randomly functionalized material. DIPP, on the other hand, shows a reduced affinity for the imprinted gel. The non-specific affinity for DIPP may be affected by differences in surface

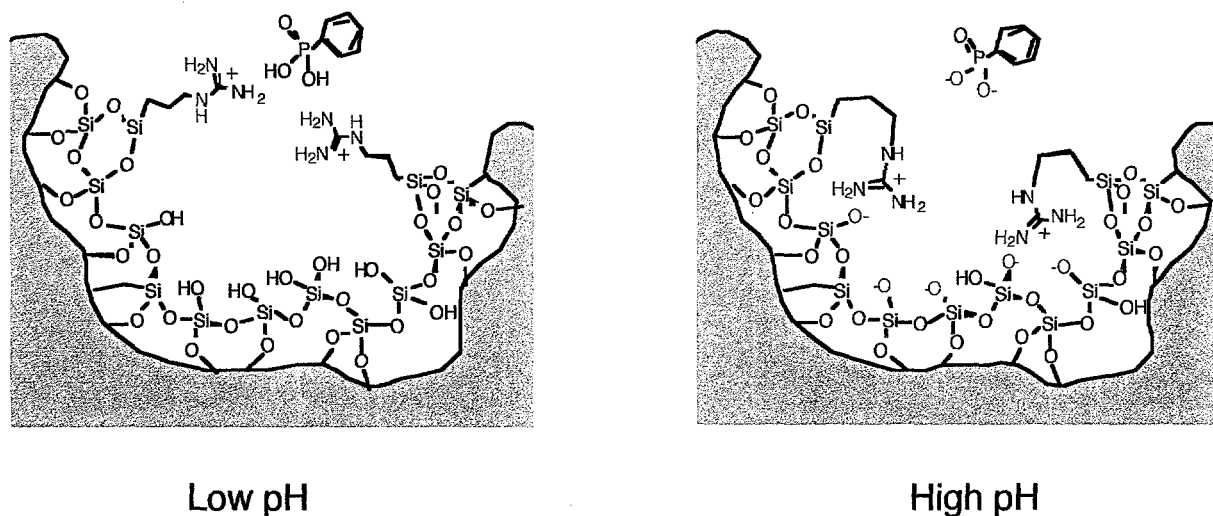

Low pH   High pH

Figure 4. Possible Scenarios for PPA Interaction with the Guanidine-Functionalized Receptor Site at Low and High pH.
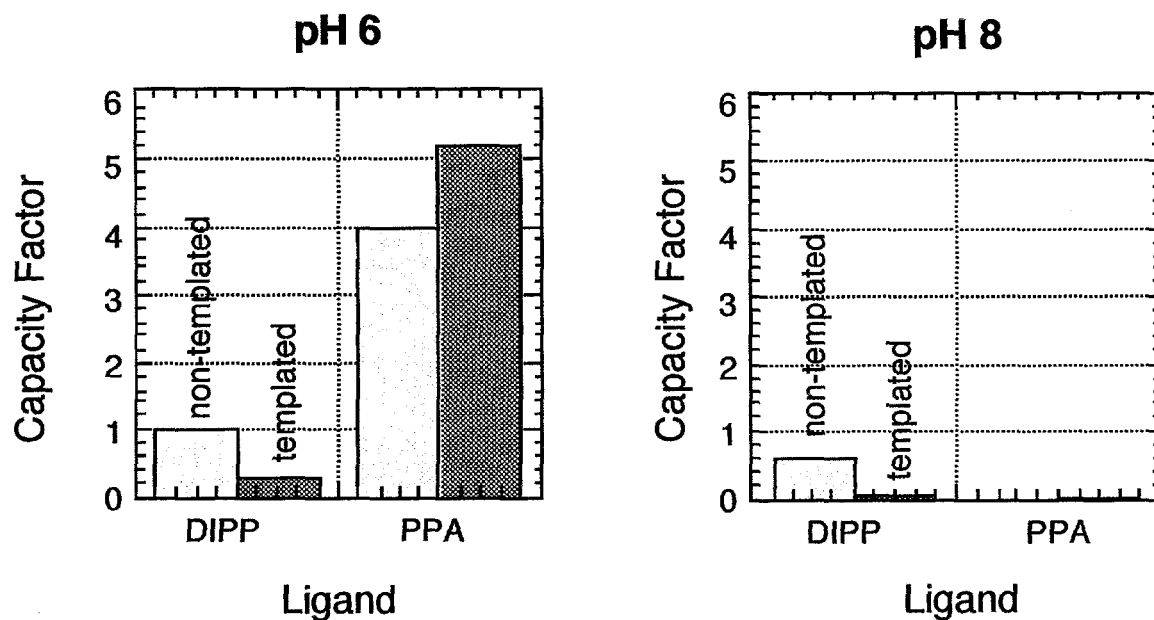

Figure 5. A Comparison of HPLC Capacity Factors of Imprinted, or Templated, vs Non-templated Guanidine-functionalized Xerogels at pH 6 and 8, Run with DIPP and PPA Substrates.

13

area which appears as a byproduct of molecular imprinting as found through BET analysis (Table I). At pH 8, there is complete loss of affinity of PPA to the xerogel. It is evident from these studies that the surface near the receptor site can play a major role in the host-guest interactions. Investigation into ways to tailor these surfaces to improve affinities as well as tune the receptor to various conditions are forthcoming.

Binding Constants. Further evaluation of the molecularly imprinted xerogels was assessed through experimental binding isotherms obtained in water at pH 5. Table II shows binding constants (K_a) and binding capacities (guanidine:substrate) for blank, 4% guanidine randomly functionalized, and 4% guanidine-PPA imprinted xerogels with phosphate (PO_4) and PPA as guest substrates. Blank xerogel was found to have negligible affinity for phosphate and PPA. On the other hand, randomly functionalized silica exhibited good binding constants for phosphate (600 M^{-1}) and PPA (1100 M^{-1}) in water. Furthermore, molecular imprinting with PPA yields an enhancement of > 2 in binding constants for both phosphate (~1500 M^{-1}) and PPA (2600 M^{-1}) compared to randomly functionalized gel. These results show that it is possible to generate refined receptor sites in sol-gel materials through a surface imprinting technique. Additional effects, such as hydrophobicity, also appear to play a role in binding of substrates to the xerogels. For example, PPA, which has a hydrophobic phenyl substituent, exhibits about a two-fold higher K_a value than the highly water soluble phosphate in both imprinted and non-imprinted functionalized materials. As has been observed with Langmuir monolayers, interfacial phenomena may promote stronger partitioning of the hydrophobic substrate to the gel bound receptor.

Table II. Binding Data of Imprinted and Non-imprinted Xerogels

% guanidine	guanidine: template	substrate	K_a (M-1)[a]	guanidine: substrate
0	none	PO_4	0	
0	none	PPA	0	
4	none	PO_4	600	1.6:1
4	none	PPA	1100[a]	2.0:1
4	2:1 PPA	PO_4	1400	2.5:1
			1600[a]	2.8:1
4	2:1 PPA	PPA	2600[a]	2.8:1

a) Data obtained by ^{31}P NMR.

Conclusions

We have shown through these initial studies that molecular imprinting in sol-gel materials can be successfully accomplished with a simple surface imprinting procedure. This method does not explicitly provide size and shape imprinting in the matrix, which is a feature of molecular imprinting. However, the method is chosen to be compatible to the sol-gel matrix, provide quantitative surface functionalization while maintaining high surface area and large pore size, and allow rapid equilibration of the receptor sites to solution. Affinities measured in aqueous solutions of phosphate and phosphonate substrates to these imprinted xerogels are one to two orders of magnitude higher than analogous small molecule receptors including pre-organized bis- and tris-guanidine receptors (8,9). The guanidine-phosphonate pairing on the gel surface shows evidence of contributions from both ionic and hydrogen bonding interactions in aqueous solution. However, the silica matrix exhibits increasing influence over the efficiency of the receptor site with rising pH due to build up of surface charge. It is anticipated that by tailoring the matrix surface the specificity of the receptors will improve and result in highly efficient molecular recognition materials for aqueous systems.

References

1) Potter, B. V. L.; Lampe, D. *Angew. Chem. Int. Ed. Engl.* **1995**, *34*, 1933.

2) Klarlund, J. K.; Guilherrne, A.; Holik, J. J.; Virbasius, J. V.; Chawla, A.; Czech, M. P. *Science* **1997**, *275*, 1927.

3) Kauffmann-Zeh, A.; Thomas, G. M. H.; Ball, A.; Prosser, S.; Cunningham, E.; Cockcroft, S.; Hsuan, J. J. *Science* **1995**, *268*, 1188.

4) *Chemical Warfare Agents: Toxicology and Treatment* Marrs, T. C.; Maynard, R. L.; Sidell, F. R., Eds.; John Wiley & Sons: New York, 1996.

5) Hirst, S. C.; Tecilla, P.; Geib, S. J.; Fan, E.; Hamilton, A. D. *Israel J. Chem.* **1992**, *32*, 105.

6) Czarnik, A. W. *SPIE - Fiber Optic Medical and Fluorescent Sensors and Applications* **1992**, *1648*, 164.

7) Deslongchamps, G.; Galán, A.; Mendoza, J. d.; Rebek, J. J. *Angew. Chem., Int. Ed. Engl.* **1992**, *31*, 61.

8) Dietrich, B.; Fyles, D. L.; Fyles, T. M.; Lehn, J.-M. *Helv. Chim. Acta* **1979**, *62*, 2763.

9) Dietrich, B.; Fyles, T. M.; Lehn, J.-M.; Pease, L. G.; Fyles, D. L. *JCS Chem. Comm.* **1978**, 934.

10) Sasaki, D. Y.; Kurihara, K.; Kunitake, T. *J. Am. Chem. Soc.* **1991**, *113*, 9685.

11) Blokzijl, W.; Engberts, J. B. F. N. *Angew. Chem. Int. Ed. Engl.* **1993**, *32*, 1545.

12) Schwabe, J. W. R. *Curr. Opin. Struct. Biol.* **1997**, *7*, 126.

13) For a comprehensive review, see: Wulff, G. *Angew. Chem. Int. Ed. Engl.* **1995**, *34*, 1812.

14) Wulff, G.; Grobe-Einsler, R.; Vesper, W.; Sarhan, A. *Makromol. Chem.* **1977**, *178*, 2817.

15) Sellergren, B.; Lepistö, M.; Mosbach, K. *J. Am. Chem. Soc.* **1988**, *110*, 5853.

16) Ramström, O.; Nicholls, I. A.; Mosbach, K. *Tetrahedron: Asymmetry* **1994**, *5*, 649.

17) Shea, K. J.; Spivak, D. A.; Sellergren, B. *J. Am. Chem. Soc.* **1993**, *115*, 3368.

18) Andersson, L. I. *Anal. Chem.* **1996**, *68*, 111.

19) Andersson, L. I.; Müller, R.; Vlatakis, G.; Mosbach, K. *Proc. Natl. Acad. Sci. U.S.A.* **1995**, *92*, 4788.

20) Calnan, B. J.; Tidor, B.; Biancalana, S.; Hudson, D.; Frankel, A. D. *Science* **1991**, *252*, 1167.

21) Cotton, F. A.; Day, V. W.; Hazen Jr., E. E.; Larsen, S.; Wong, S. T. K. *J. Am. Chem. Soc.* **1974**, *96*, 4471.

22) Raman, N. K.; Anderson, M. T.; Brinker, C. J. *Chem. Mater.* **1996**, *8*, 1682.

23) Morihara, K.; Kurihara, S.; Suzuki, J. *Bull. Chem. Soc. Jpn.* **1988**, *61*, 3991.

24) Wulff, G.; Heide, B.; Helfmeier, G. *J. Am. Chem. Soc.* **1986**, *108*, 1089.

25) Heilmann, J.; Maier, W. F. *Angew. Chem. Int. Ed. Engl.* **1994**, *33*, 471.

26) Dickey, F. H. *Proc. Natl. Acad. Sci. USA* **1949**, *35*, 227.

27) Bernatowicz, M. S.; Xu, Y.; Matsueda, G. R. *J. Org. Chem.* 1992, *57*, 2497.

28) Brinker, C. J.; Keefer, K. D.; Schaefer, D. W.; Ashley, C. S. *J. Non-Crystal. Solids* **1982**, *48*, 47.

29) *Sol-Gel Science: The Physics and Chemistry of Sol-Gel Processing* Brinker, C. J.; Scherer, G. W., Eds.; Academic Press, Inc.: San Diego, 1990.

30) Prakash, S. S.; Brinker, C. J.; Hurd, A. J.; Rao, S. M. *Nature* **1995**, *374*, 439.

Appendix

Molecular Modeling of Phosphonate Receptor Site

Computer modeling was used to garner insights into phosphonate and phosphate molecular recognition in biological systems revealing key functional group interaction points used in nature. The functionality were isolated and transposed into a model synthetic receptor in a silica matrix and the lowest energy structure in the presence of a phosphonate substrate identified. These studies confirmed the viability of our approach towards a synthetic receptor as we found the matrix coalesced around the phosphate substrate with high host-guest binding energy.

Molecular modeling studies were performed to aid in the design of biomimetic molecular recognition materials that bind phosphate and phosphonate ligands. There are two design goals: 1) to examine phosphonate and phosphate binding in known biological systems and identify the key molecular recognition features, and 2) to build 3-D molecular models of a proposed receptor site in a synthetic material to evaluate possible interactions based on these key features. Phosphonate binding in natural and engineered materials was studied in three steps. First, we culled the protein data bank for suitable phosphate binding structures. Next, we evaluated the binding energy of these using a combined molecular mechanics/Monte Carlo technique. Finally, we suggested the positions of the engineered binding pocket atoms based on the previous results and ran Molecular Dynamics simulations of phosphate ion and a phosphonate molecule in a model aerogel.

Brookhaven's Protein Data Bank was searched for 'phosphate' (256 responses) and 'phosphonate' (30 entries) binding proteins. These structures were downloaded and investigated using MSI's Insight molecular modeling program. The binding pocket was determined to be a 20Å radius sphere surrounding the phosphate ligand (i.e., phosphate ion, NAD+, ATP, ADP, AMP). For all simulations we used the USF's Amber forcefield. The interactions included partial coulombic charges and van der Waals interactions (100Å cutoff) which combine to approximate hydrogen bonds. A list of structures used in the final analysis were tabulated along with pertinent surface chemical properties. Eighteen of these which had the strongest intermolecular energy for the different binding agents were used in further binding analysis. MSI's docking module was then used to compute the binding energy of the phosphate ligand. This computer experiment randomly chooses positions of the bound molecule and evaluates the energy. Finally, the binding pockets were analyzed for the prevailing amino acid residues that lined the adsorption site. Some of the striking features found in the initial characterization of these proteins were the large number of hydrogen bonds (as many as three per phosphate oxygen) and their unusual tightness. Key functionality at the receptor site include guanidinium from arginine, amine from lysine, imidazole from histidine, amide hydrogens from the protein backbone, and hydroxyls from serine and water. A representative example is shown in Figure A-1 of the phosphate-phosphotransferase complex.

Electrostatics of the protein environment showed larger positive potential near the negatively charged phosphate oxygen compared to where the neutral (protonated) phosphate oxygens bind. Past mutant protein studies have shown that modifying this potential can alter which phosphate species (monobasic vs. dibasic) preferentially binds to a protein.
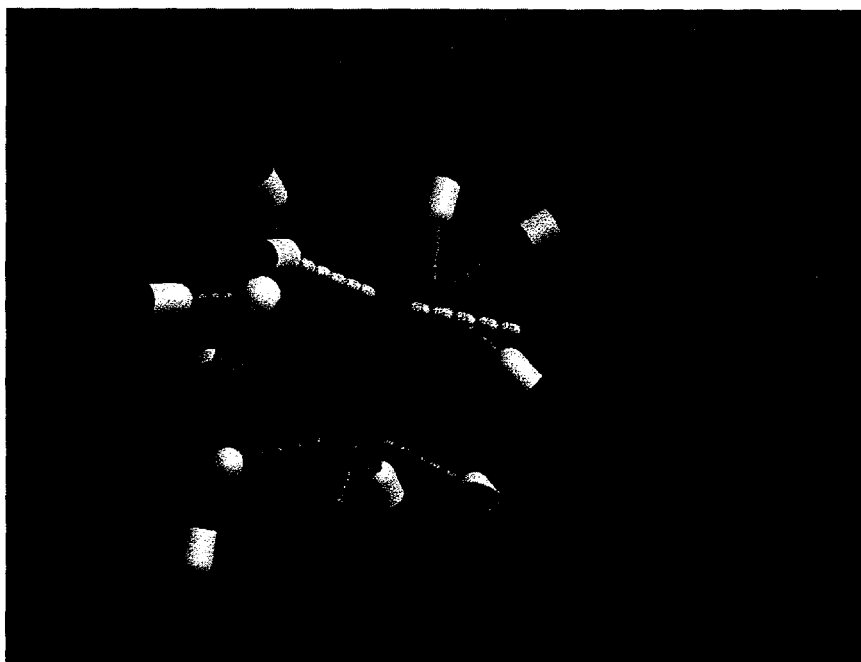

Figure A-1. Phosphate-phosphotransferase complex binding site.

In an effort to examine the proposed synthetic receptor we modeled it in 3-D space as an isolated site and as incorporated into a silicate matrix. In the isolated site our goal was to evaluate combinations of functional groups which maximize the number of possible interactions while minimizing steric and electrostatic repulsions. The evaluation consists of examining the possible spatial orientations that exist for a given set of groups. We used distances and angles from known protein-substrate complexes to help in the functional groups placement. We assumed the amines would maximally bind with the phosphate, and threw out sterically overlapping arrangements. A minimized structure was obtained showing high convergence of two guanidines and the anthracene diamine to the phosphate substrate. The energy minimized structure is shown in Figure A-2.

Modeling of the synthetic receptor in the silicate matrix was performed using Molecular Dynamics on a time domain of 100 picoseconds using a time step of one femtosecond. The functional group used was the guanidinium which was placed randomly in a porous silica model grown by cluster-cluster aggregation, based on experimental ^{29}Si NMR and small angle X-ray
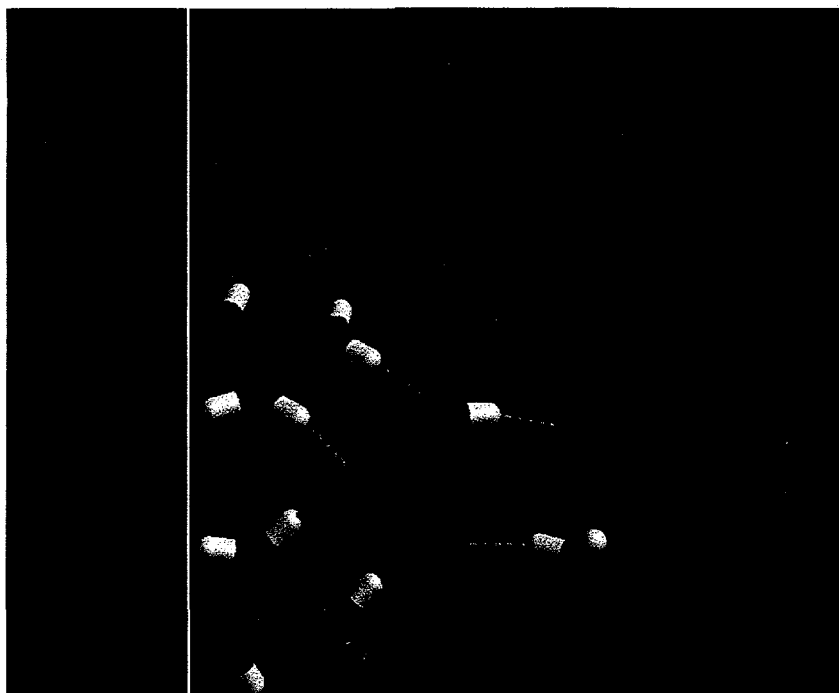
Figure A-2. Proposed synthetic receptor site in 3-D space.

scattering results. A phosphate or phosphonate substrate was placed near the matrix surface and the system allowed to energy minimize (Figure A-3). The extraordinary result is that the guanidine functionality collapsed around the phosphate, or phosphonate, ion as indicated by the pair correlation functions between nitrogen atoms and phosphate atoms. This suggests that a siloxane matrix functionalized with guanidinium groups would have good probability in forming receptor sites with high molecular recognition for phosphate or phosphonate ion.
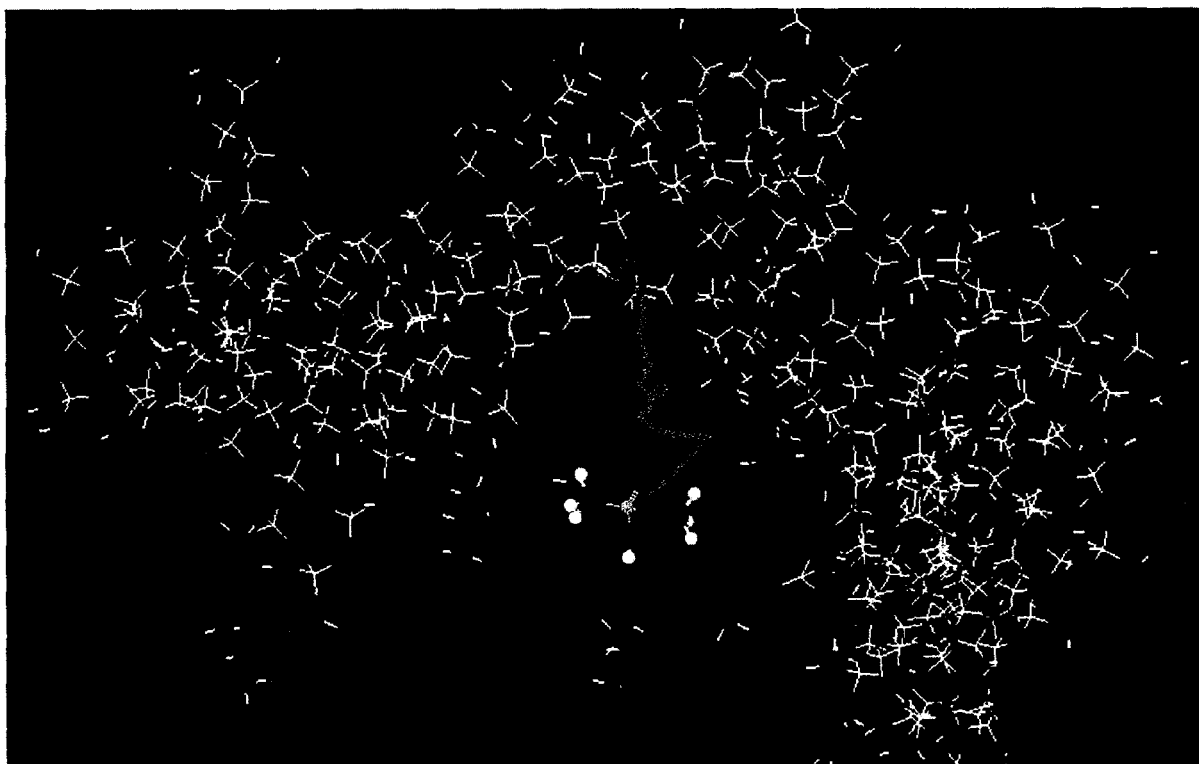
Figure A-3. Model of a silicate matrix randomly functionalized with guanidines in a molecular dynamics simulation with a phosphonate substrate. The blue line shows the trajectory of the substrate ending near a multi-guanidinium receptor site.

DISTRIBUTION:

3			Prof. Kenneth J. Shea University of California, Irvine Chemistry Department Irvine, CA 92717
1			Dr. Daniel Rush University of California, Irvine Chemistry Department Irvine, CA 92717

8	MS	1407	D. Sasaki
1		1349	C. J. Brinker
1		1349	C. Ashley
1		1407	T. Alam
1		1407	R. Assink
1		1425	A. Ricco
1		1425	M. Butler
1		9214	J. Schoeniger
1		9214	D. Roe
1		0727	P. Pohl
1		1407	R. Clough
1		0188	C. E. Meyers, LDRD Office
1		9018	Central Technical Files, 8940-2
5		0899	Technical Library, 4414
2		0619	Review & Approval Desk, 12690 For DOE/OSTI